GeoScienceWorld
Lithosphere
Volume 2021, Article ID 3765068, 15 pages
https://doi.org/10.2113/2021/3765068

Lithosphere

Research Article

Experimental Study on the EOR Performance of Imbibition and Huff and Puff in Fractured Tight Oil Reservoirs

Zilin Zhang,[1] Bo Huang,[1] Liang Zhang,[2,3] Guangqing Zhou,[1] Yanhui Liu,[1] Chenyang Li,[2] and Dianfa Du[2,3]

[1]*Shengli Oilfield, Sinopec, Dongying 257000, China*
[2]*School of Petroleum Engineering, China University of Petroleum (East China), Qingdao 266580, China*
[3]*Key Laboratory of Unconventional Oil & Gas Development, China University of Petroleum (East China), Qingdao 266580, China*

Correspondence should be addressed to Zilin Zhang; cyyylzzl@163.com and Liang Zhang; zhlupc@upc.edu.cn

Received 16 April 2021; Accepted 8 June 2021; Published 6 September 2021

Academic Editor: Xixin Wang

Injection of imbibition fluids or CO_2 during hydraulic fracturing is an effective stimulation method for tight oil reservoirs. Selecting appropriate agents is significant to optimize the integrated scheme of fracturing and production in tight oil reservoirs. In this study, a series of lab experiments, including spontaneous imbibition, dynamic imbibition, and huff and puff, were carried out using real tight cores, water absorption apparatus, and core flooding equipment. The EOR performances of imbibition fluids and CO_2 in fractured tight cores were compared. The mass transfer of imbibition fluids and CO_2 in tight oil reservoirs and its influence on the sweeping volume and EOR mechanisms were discussed. The results show that (1) the spontaneous imbibition rate of imbibition fluids in tight cores is slow, and the oil recovery factor by spontaneous imbibition in cracked cores is relatively high, up to 13.42%. (2) In the dynamic imbibition experiments, the final oil recovery by CO_2 injection was significantly higher than that by injecting imbibition liquids. Because of the excellent miscibility effect of CO_2, oil production by CO_2 injection mainly occurred in the primary displacement stage. Comparatively, the EOR effect of imbibition fluids mainly played its role during production after well shut-in, which can increase the oil recovery factor by 7.35%-11.64%. (3) The influence of the huff and puff mode of CO_2 on EOR performance is greater than that of imbibition fluids due to its more sensitive compressibility and mass transfer rate. Generally, a high oil recovery factor can be obtained if the depletion production is conducted first, and a huff and puff operation is followed. (4) Comprehensively understanding the mass transfer characteristics of CO_2 and imbibition fluids in tight oil reservoirs can guide the fracturing parameter design, such as the order of fracturing fluid slugs, the optimal soak time, and fracture spacing.

1. Introduction

Tight oil reservoirs have poor reservoir physical properties with large heterogeneity and low porosity and permeability. Hydraulic fracturing is the commonly used stimulation method to improve oil recovery in tight oil reservoirs. However, there are still problems such as low production rate, rapid production decline, and poor economic benefits [1–4]. Hence, new fluids such as imbibition fluids and gases (e.g., CO_2) are considered to inject into tight oil reservoirs for further enhanced oil recovery (EOR) by huff and puff [5–10]. To reveal the EOR mechanisms and performance of different oil displacement agents in tight oil reservoirs is significant for the integrated scheme optimization of fracturing and production.

At present, there have been a lot of studies on the stimulation mechanisms of imbibition fluids and CO_2 in tight oil reservoirs [11–27]. Imbibition is one of the main methods of oil production in tight oil reservoirs, and the main driving force of imbibition is capillary force. In the process of reservoir development, the injected fluid is imbibed into the matrix to replace the crude oil, which can effectively improve the development effect of tight reservoirs. Therefore, many scholars have conducted in-depth research on the mechanism of imbibition, experimental methods, and influencing factors [28]. For the imbibition mechanisms, there have been

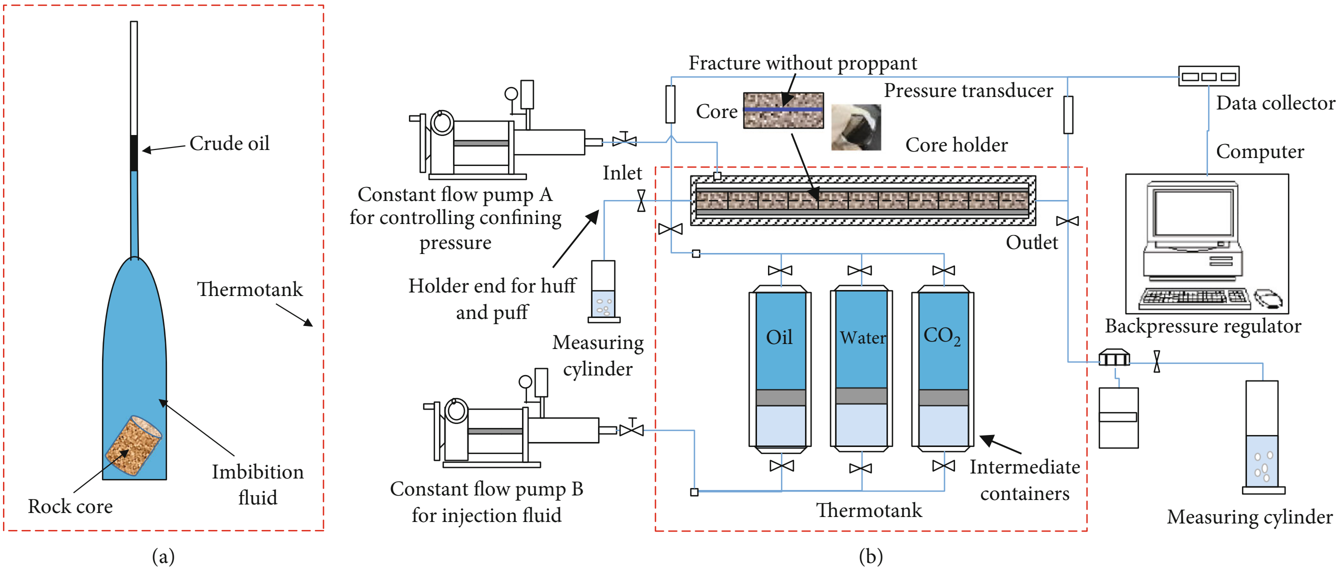

Figure 1: Schematic diagram of the equipment used in experiments: (a) water absorption apparatus; (b) core flooding equipment for dynamic imbibition and huff and puff.

relatively mature theories [11, 12]. In tight oil reservoirs, the capillary force inducing fluid imbibition is strong, but the seepage resistance of fluid is also large because of the low permeability. How to use the existing imbibition theory to develop tight oil reservoirs effectively is an important research topic. The current researches about fluid imbibition in tight oil reservoirs are mainly focused on the imbibition mechanism in the fracture network system at a microscale [13–17] as well as the screening and synthesis of excellent additives to improve the EOR function of fracturing fluids [18–22]. For the selection of imbibition fluids, nanoparticle fluids have excellent performance and good application prospects. However, due to its high surface energy, agglomeration is prone to occur, resulting in poor water dispersibility. By modifying the nano-SiO_2 fluid, the modified nanoparticle fluid with good dispersion properties is obtained. Compared with the unmodified nano-SiO_2 fluid, the modified nanoparticle fluid has a good effect of changing the wettability of the rock, which can make the lipophilic surface hydrophilic, and can reduce the interfacial tension and increase the imbibition recovery rate [29]. For the EOR mechanisms of CO_2, there have been in-depth understandings in conventional oil reservoirs. In view of the excellent swelling, viscosity reduction, and mass transfer characteristics of CO_2, CO_2 can be used as a fracturing fluid, an additive, or an oil displacement agent for huff and puff and flooding [23–27]. To sum up, imbibition fluids and gases with CO_2 as the representative have been the commonly used fluids for integrated fracturing and production in tight oil reservoirs. However, the phase state and EOR mechanisms of these two kinds of fluid are quite different, which are often studied separately. In the fracture system of tight oil reservoirs, the front locations which these two kinds of fluid can reach for oil recovery are different. To accurately understand the EOR performance and mass transfer characteristics of these two kinds of fluids is beneficial for optimizing the fracturing fluid and oil displacement agent for tight oil reservoir development.

In this study, a series of comparative experiments of imbibition fluids and CO_2 were conducted, including spontaneous imbibition, dynamic imbibition, and huff and puff using real tight cores with fractures, water absorption apparatus, and core flooding equipment. The EOR performance of imbibition fluids and CO_2 by imbibition effect and huff and puff operation in tight oil rocks was evaluated. The mass transfer of imbibition fluids and CO_2 in tight oil reservoirs and its influence on the sweeping volume and EOR performance were discussed.

2. Experimental Equipment and Methods

2.1. Experimental Equipment. The water absorption apparatus was used for spontaneous imbibition experiments, and the core flooding equipment was used for dynamic imbibition and huff and puff experiments. As shown in Figure 1(a), the water absorption apparatus comprises the upper cover with a slim vertical tube and the lower cup. During experiments, the tight core saturated with crude oil is placed in the lower cup, and the imbibition fluid is injected into the water absorption apparatus. When crude oil is produced from the core by the imbibition effect, it will accumulate in the slim tube under buoyancy force. The produced oil volume can be determined by reading the scale line on the slim tube.

The core flooding equipment used in experiments is shown in Figure 1(b). This equipment mainly includes (1) two constant flow pumps used for fluid injection and confining pressure maintenance, respectively; (2) three intermediate containers used to hold crude oil, injected water/imbibition liquid, and CO_2 gas, respectively; (3) core holder and backpressure regulator used to keep cores at designated porous pressure and confining pressure (its maximum working pressure and temperature are 50 MPa and 150°C, respectively); (4) thermotank used to maintain the core holder and intermediate containers at a designated

Table 1: Main ion composition of formation water in block Y222.

Cation (mg/l)			Anion (mg/l)		Salinity (mg/l)	Water type
Na^++K^+	Ca^{2+}	Mg^{2+}	Cl^-	HCO_3^-		
18714	1407	142	31358	669	52290	$CaCl_2$

Table 2: Properties and usage of each core used in experiments.

No.	Core	L (cm)	D (cm)	K (mD)	φ (%)	Status	Spontaneous imbibition	Dynamic imbibition	Huff and puff
1	27#	5.54	2.50	—	2.70	Cracked	✓		
2	23#	6.14	2.50	—	6.60	Cracked	✓		
3	26#	5.48	2.50	—	3.28	Cracked	✓		
4	29#	4.18	2.50	—	3.60	Cracked	✓		
5	B244	6.00	2.50	1.132	7.77	Complete	✓		
6	A11	5.15	2.50	0.013	4.02	Complete	✓		
7	C7	5.12	2.49	0.387	6.52	Complete	✓	✓	
8	D4	5.87	2.51	0.606	12.80	Complete	✓		
9	B154-3	5.95	2.48	0.854	12.64	Complete	✓		
10	A10	4.47	2.48	0.168	7.36	Complete		✓	
11	B14	4.18	2.48	0.012	3.86	Complete			✓

temperature during experiments; and (5) pressure sensors, data collector, and computer used to measure the pressures at the front and back ends of the core holder.

2.2. Experimental Materials

(1) *Crude Oil*. The degassed crude oil from the tight oil block Y222 in Shengli Oilfield, China, was used. The density and viscosity of the crude oil at the surface (50°C) are 0.8421 g/cm^3 and 9.4 mPa·s, respectively, while its formation density and viscosity are 0.7217 g/cm^3 and 1.17 mPa·s, respectively

(2) *Formation Water*. the formation water used in experiments was prepared according to the ion composition of the formation water in block Y222, as shown in Table 1

(3) *Gas*. Gas used is CO_2 gas with high purity of 99.99%

(4) *Imbibition Liquids*. Three types of imbibition liquids were used with code names SX-1, SX-2, and SX-3, respectively. By using the modifier to modify the nano-SiO_2, the modifier can chemically react with the groups on the surface of the nano-SiO_2 to improve the ability to change the wettability of the rock surface. The three imbibition liquids are three aqueous solutions of modified nano-SiO_2 particles with different abilities to change the wettability of the rock surface. The initial concentration was 6 wt% and diluted to 0.1 wt% for use in experiments

(5) *Real Cores*. Eleven real cores were sampled from block Y222 which is a tight sandy conglomerate oil reservoir. Before experiments, all cores were cleaned using the Soxhlet extractor and benzene. The porosity and permeability of cores were measured by the saturating-weighing and water flooding methods. The core properties and usage in experiments are shown in Table 2

2.3. Experimental Procedures

2.3.1. Spontaneous Imbibition Experiment. The spontaneous imbibition experiment was designed to verify the static imbibition and oil displacement capacity of imbibition liquids and formation water in tight cores. The specific experimental procedures are as follows:

(1) Use Soxhlet extractor to clean the cores, weigh the core mass, and saturate the cores with crude oil at a temperature higher than 80°C using the core flooding equipment (for complete cores) or by the vacuuming method (for cracked cores). When the complete core is saturated, the core is saturated after 5-10 times the pore volume of crude oil is continuously injected into the core; when the cracked core is saturated by vacuuming, the core is saturated after the cracked core mass no longer increases. After the cores are saturated with oil, wipe the crude oil adhering to the core surface, weigh the core mass again, and calculate the saturated oil mass and volume

(2) Put one core in the water absorption apparatus and inject the imbibition liquid or formation water into the apparatus until the liquid surface reaches the middle of the slim tube on the top; cover a piece of plastic preservative film on the outlet of the slim tube to prevent water evaporation

(3) Put the water absorption apparatus in the thermotank to maintain at a constant temperature for imbibition, record the height of the crude oil in the slim tube every 0.5-4 h, calculate the oil volume replaced by imbibition fluid in the core, and plot the oil production and recovery factor with time

2.3.2. Dynamic Imbibition Experiment. The dynamic imbibition experiment was designed to explore the imbibition and displacement performance of various fluids in the fractured tight cores at high pressure and high temperature. The specific experimental procedures are as follows:

(1) Saturate crude oil into the complete tight cores using the flooding method and calculate the statured oil volume in the cores according to the change of core mass before and after displacement, cut the cores into half along the axis, put the spliced cores into the core flooding equipment to saturate oil further, and correct the saturated oil volume

(2) Set the backpressure and confining pressure of the core holder, inject the imbibition liquid or CO_2 into the core at the front end until no more oil is produced at the back end, stop the injection, and shut in the valves of the core holder for a soaking time; then, open valves and continue to inject imbibition liquid or CO_2 again until no oil is produced

(3) Repeat the injection and soaking several times until no oil is produced

(4) During the experiment, continuously monitor the pressure at the front and back ends of the core holder and calculate the displacement pressure difference and record the injected and produced amount of oil and water to calculate the saturation and oil recovery factor in the cores

2.3.3. Huff and Puff Experiment. The huff and puff experiment was designed to assess the EOR performance of huff and puff of imbibition liquids and CO_2 in fractured cores at high pressure and high temperature. The experimental procedures are similar to those of the dynamic imbibition experiment except the fluid injection and production mode. In the huff and puff experiment, the backpressure of the core holder is kept at a constant value. The imbibition liquids and CO_2 are injected and produced at the same end (front end) of the core holder. Similarly, the pressure of the core holder and the fluid injection and production are also recorded to analyze the EOR performance of huff and puff.

2.4. Experimental Schemes. The experimental scheme of spontaneous imbibition is shown in Table 3. Ten cases were carried out at 80°C and atmospheric pressure using nine cores to test the static imbibition performance of formation water and three types of imbibition fluids. The imbibition time was 50-96 h when the imbibition effect tended to be stable.

Table 4 shows the experimental scheme of dynamic imbibition. Three cases were designed to test the dynamic imbibition performance of formation water, CO_2, and imbibition liquid SX-2. Two cores with close properties were cut into half to simulate the fracture without proppant. The experimental temperature was 80°C. The backpressure and confining pressure of the core were 10 MPa and 15 MPa, respectively (the effective stress on the core was 5 MPa). The fluid injection rate was 0.05 ml/min. Two cycles were conducted, and the soaking time was 12-24 h.

Table 3: Experimental scheme of spontaneous imbibition.

No.	Core	φ (%)	K (mD)	Status	Imbibition fluid
1	27#	2.70	—	Cracked	Formation water
2	23#	6.60	—	Cracked	Formation water
3	B244	7.77	1.132	Complete	Formation water
4	26#	3.28	—	Cracked	Imbibition fluid SX-1
5	A11	4.02	0.013	Complete	Imbibition fluid SX-1
6	29#	3.60	—	Cracked	Imbibition fluid SX-1
7	C7	6.52	0.387	Complete	Imbibition fluid SX-2
8	D4	12.80	0.606	Complete	Imbibition fluid SX-2
9	B154-3	12.64	0.854	Complete	Imbibition fluid SX-2
10	A11	4.02	0.013	Complete	Imbibition fluid SX-3

As shown in Table 5, seven cases in huff and puff experiments were designed. The same fractured core (B14) without proppant was used in the experiments. The soaking time of huff and puff was 24 h, and only one cycle of huff and puff was carried out in each case. The experimental temperature, pressure, and injection rate were the same as those in the dynamic imbibition experiments.

3. Experimental Results and Analysis

3.1. Spontaneous Imbibition Performance of Different Imbibition Liquids at Atmospheric Pressure. The experimental results of spontaneous imbibition at 80°C and atmospheric pressure are shown in Table 6 and Figure 2. In general, the imbibition performance of various fluids ranks in the order of SX-2>SX-3>SX-1>formation water. The imbibition liquid SX-2 has the best imbibition effect, which can contribute an oil recovery factor up to 13.416% (case 8). When the formation water was used as an imbibition fluid, the oil recovery factor was only 3.965%-5.506% (cases 1-3). This is because the imbibition liquid SX-2 has the best interface properties, and the nanoparticles in the imbibition liquid SX-2 are adsorbed on the surface of the pores, reducing the wetting angle and enhancing the capillary force. Therefore, it is of great significance to select imbibition fluids for EOR. The cores with large porosity and permeability usually have a high imbibition rate, which can reach stability within 24 h. Relatively, the tighter cores require a longer imbibition time (60-100 h) to reach stability. Compared with the complete cores, the cracked cores have a better imbibition effect (such as cases 4-6) because the imbibition liquid can contact more core matrix through the fractures to displace more crude oil out. On the whole, the core porosity and oil recovery factor present an excellent positive correlation.

Table 4: Experimental scheme of dynamic imbibition.

No.	Injected fluid	Core	Injection mode	Injection volume	Soaking time (h)	Cycle number	Boundary condition
1	Formation water	A10	Displacement -soak alternation	Until no oil produced	12-24	2	Constant pressure
2	CO_2	A10					
3	Imbibition liquid SX-2	C7					

Table 5: Experimental scheme of huff and puff.

No.	Injected fluid	Timing of huff and puff	Injection volume
1	Formation water	After depletion	To original pressure + 0.2 PV
2	CO_2	After depletion	To original pressure
3	CO_2	After depletion	To original pressure + 0.2 PV
4	CO_2	Direct huff and puff	0.2 PV
5	Imbibition fluid SX-2	After depletion	To original pressure
6	Imbibition fluid SX-2	After depletion	To original pressure + 0.2 PV
7	Imbibition fluid SX-2	Direct huff and puff	0.2 PV

Table 6: Experimental results of spontaneous imbibition.

No.	Core	Saturated oil (ml)	Imbibition liquid	Imbibition time (h)	Replacement oil volume (ml)	Oil recovery factor (%)	Core status
1	27#	0.588	Formation water	60	0.029	4.932	Cracked
2	23#	1.589	Formation water	96	0.063	3.965	Cracked
3	B244	4.831	Formation water	60	0.266	5.506	Complete
4	26#	0.705	Imbibition liquid SX-1	70	0.054	7.660	Cracked
5	A11	0.822	Imbibition liquid SX-1	96	0.056	6.813	Complete
6	29#	0.590	Imbibition liquid SX-1	50	0.049	8.305	Cracked
7	C7	1.300	Imbibition liquid SX-2	60	0.120	9.231	Complete
8	D4	2.974	Imbibition liquid SX-2	80	0.399	13.416	Complete
9	B154-3	2.916	Imbibition liquid SX-2	66	0.388	13.306	Complete
10	A11	0.822	Imbibition liquid SX-3	60	0.069	8.456	Complete

3.2. Comparison of Dynamic Imbibition Performance of Imbibition Liquid and CO_2. The experimental results of dynamic imbibition are shown in Figures 3–5. As shown in Figure 3, when the formation water was used as the imbibition fluid, the experimental results show that the oil recovery factor during the initial water displacement was only 23.28%, while the oil recovery factor was enhanced by 5.4% and 4.78% in the subsequent two times of soaking for imbibition and displacement, respectively; during production after soaking, the water cut decreased first but increased to 100% quickly. In the initial water displacement, the peak of displacement differential pressure was large, close to 3 MPa, while in the subsequent second and third water displacement stages, the peaks of displacement differential pressure gradually decreased in turn. Besides, it can also be observed that the pressure in the core decreased and tended to be stable (lower than 0.35 MPa) during the soaking stages under the effect of imbibition.

When the best SX-2 was used as the injection fluid, the oil recovery factor can reach 34.93% during the initial displacement, as shown in Figure 4. It can be further enhanced by 11.64% and 7.35% in the subsequent two times of soaking and displacement processes, respectively, which indicates the excellent imbibition effect of SX-2. Because the imbibition liquid SX-2 has a stronger imbibition effect than formation water, the drop and fluctuation frequency of water cut are higher than formation water when the well is opened after soaking. For the displacement differential pressure, it is similar to that in the case of formation water injection.

As shown in Figure 5, when CO_2 was used as the injection fluid, an oil recovery factor as high as 54.22% was obtained in the initial displacement stage under the displacement and miscibility effects. In the subsequent two times of soaking and displacement, the oil recovery was further increased by 8.83% and 5.04%, respectively. During the initial CO_2 displacement, the peak of displacement differential pressure

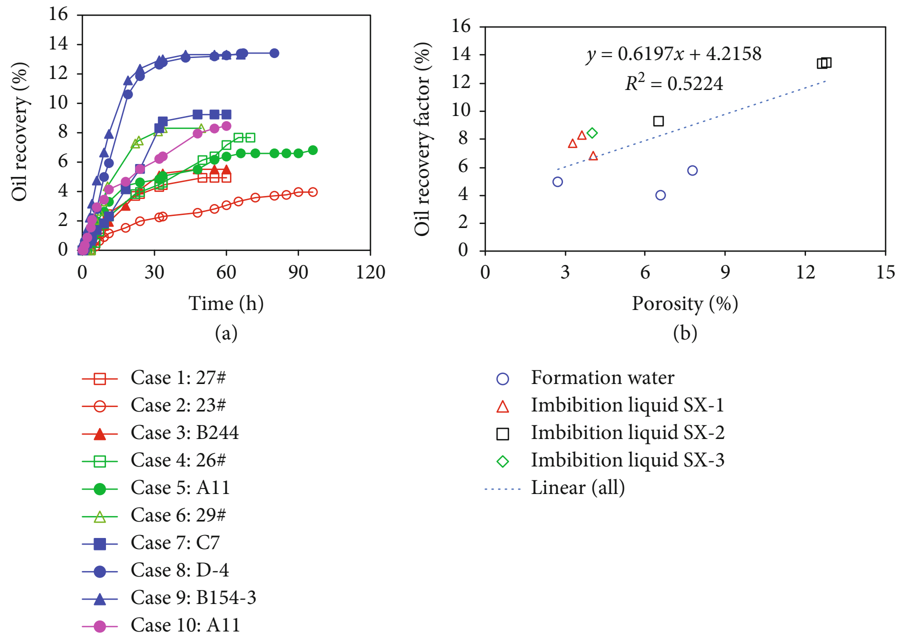

Figure 2: Oil recovery factor of different cores by spontaneous imbibition ((a) red line: formation water; green line: imbibition liquid SX-1; blue line: imbibition liquid SX-2; pink line: imbibition liquid SX-3; solid color filled mark: complete core; unfilled mark: cracked core): (a) oil recovery factor of cores with time; (b) correlation between oil recovery factor and porosity.

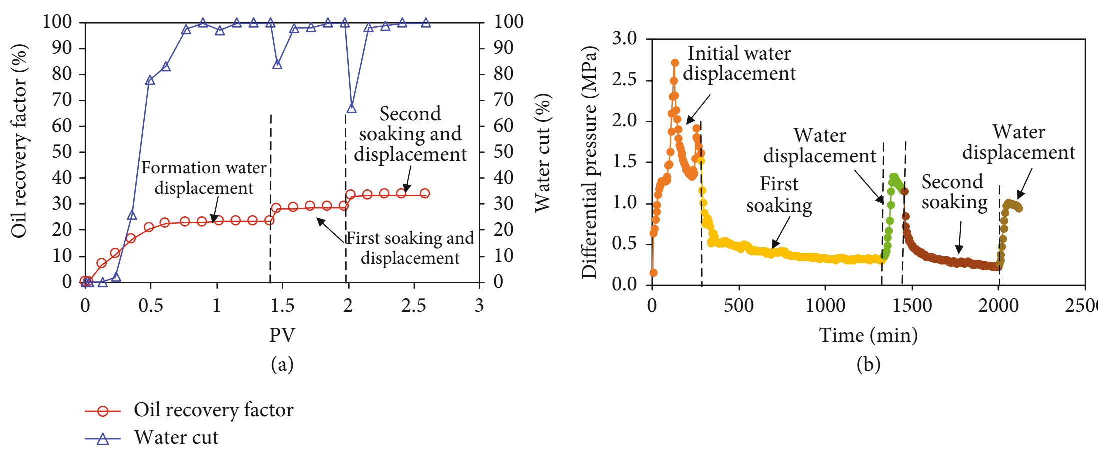

Figure 3: Production performance when formation water was injected for dynamic imbibition: (a) oil recovery factor and water cut; (b) displacement differential pressure.

was large. However, the peak of displacement differential pressure between the second and the third CO_2 displacement is basically the same and smaller than the initial stage. Compared with the water injection, the maximum displacement pressure difference of CO_2 was smaller, only 1.3 MPa. This is because oil-water two-phase flow occurs when the imbibition liquid is injected, the irreducible water saturation and residual oil saturation are large, the two-phase flow area in the phase permeability curve is narrow, and the seepage resistance of two-phase flow has a higher peak value with the increase of water saturation. When CO_2 is injected, gas-water two-phase flow occurs mainly, the residual oil saturation is low, the two-phase flow area is wider, and the seepage resistance distributes smoothly as the gas saturation increases. Due to the CO_2's high compressibility and excellent swelling effect on the crude oil, the decrease of pressure in the core during the soaking stage is smaller than that when imbibition liquid SX-2 and formation water were injected.

The experimental results of these three dynamic imbibition cases are summarized in Table 7. By comparison, it can be seen that the displacement and imbibition performance of formation water was the worst. The final oil recovery factor was only 33.46%. In contrast, the CO_2 displacement and crude

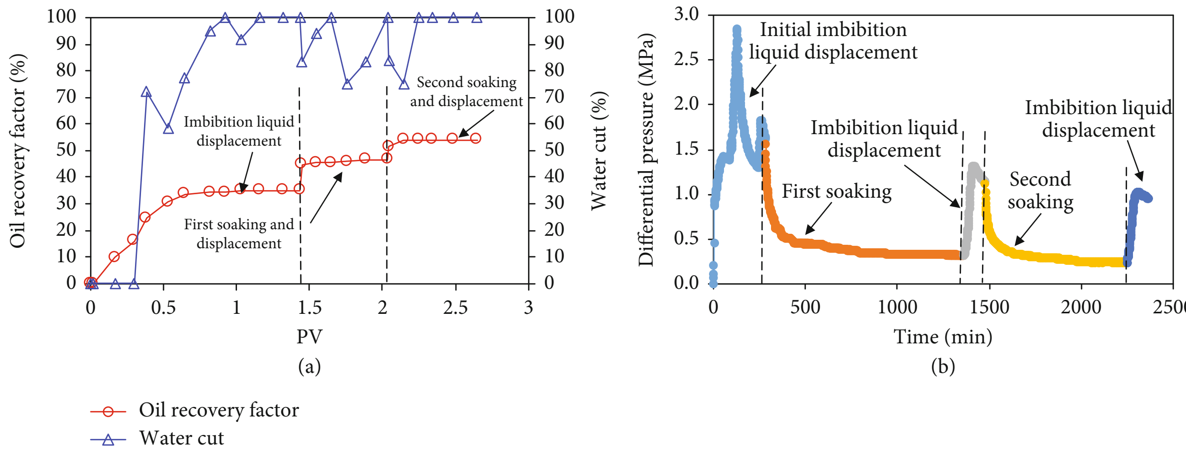

FIGURE 4: Production performance when imbibition liquid SX-2 was injected for dynamic imbibition: (a) oil recovery factor and water cut; (b) displacement differential pressure.

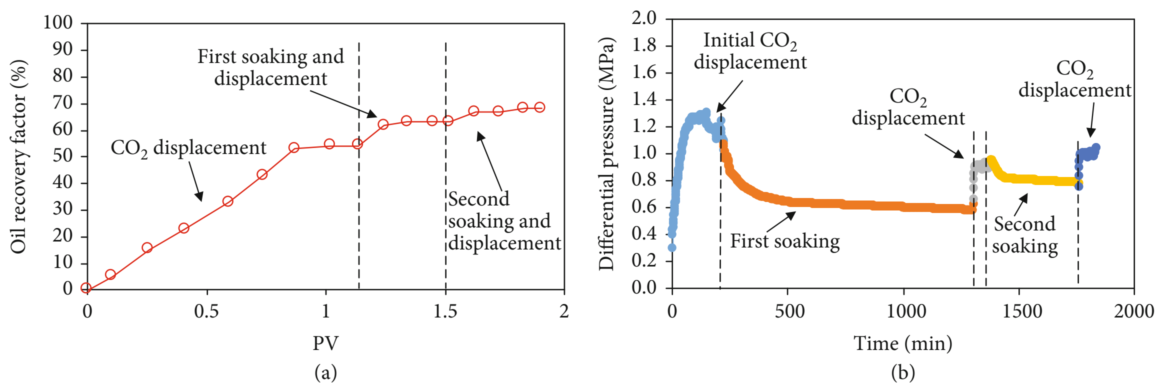

FIGURE 5: Production performance when CO_2 was injected for dissolution and swelling: (a) oil recovery factor; (b) displacement differential pressure difference.

oil swelling presented a better performance, which can achieve a higher final oil recovery factor up to 68.10%, 14.18% larger than that in the case of imbibition fluid SX-2.

It should also be noticed that when the imbibition liquid SX-2 was used for dynamic imbibition, the produced fluid has a water cut. The oil replaced by the imbibition liquid during the soaking time was produced quickly associated with a large amount of water. This demonstrates the significant imbibition effect of the imbibition liquid SX-2 for EOR. Besides, when CO_2 was used for displacement and dissolution-swelling, there is no water cut problem. The fluid produced at the outlet of the core holder was mainly crude oil. Due to the large compressibility and solubility of CO_2 in crude oil, the oil was produced slowly during the production stage after soaking.

3.3. Comparison of Huff and Puff Performance of ImbibitionLiquid and CO_2. The experimental results of huff and puff in the fractured tight core are shown in Figures 6–9. Case 1 is a blank experiment in which the injected fluid is formation water. As shown in Figure 6, the huff and puff experiment of formation water experienced the following steps: initial production by pressure depletion➔pressure recovery by injecting formation water➔continuous constant pressure injection of 0.2 PV formation water ➔ soaking for 24 h➔ production by depressurization. In the initial depletion production, the oil recovery factor was 16.99%. After the huff and puff of formation water, the recovery was increased by 4.24%, reaching 21.23%, and associated with a water cut of 86.67-98.84% in the produced liquid.

As shown in Figure 7, cases 2 and 5 used the same huff and puff mode, similar to case 1 except for the additional injection of 0.2 PV. It can be seen that when CO_2 was used for the huff and puff, the oil recovery factor in the initial depletion production was 17.62%. After CO_2 huff and puff, the oil recovery factor was increased by 15.07%, reaching 32.70%. Comparatively, when the imbibition liquid SX-2 was used for the huff and puff, the oil recovery factor was only improved by 8.70% from 19.53% in the depletion production to 28.24% after huff and puff. The water cut in the produced fluid during the puff process increased from 40% to 94% gradually.

Cases 3 and 6 took the same experimental procedures in case 1. As shown in Figure 8, when CO_2 was injected for huff and puff, the finial oil recovery factor can reach 40.34%, which is 19.75% higher than that in the initial depletion

Table 7: Summary of dynamic imbibition experimental results.

No.	Injected fluid	Initial oil volume (ml)	Stage cumulative oil (ml)			Stage oil recovery (%)			Final oil recovery factor (%)
			Initial displacement	1st soaking for imbibition	2nd soaking for imbibition	Initial displacement	1st soaking for imbibition	2nd soaking for imbibition	
1	Formation water	8.16	1.90	0.44	0.39	23.28	5.4	4.78	33.46
2	Imbibition fluid SX-2	8.16	2.85	0.95	0.6	34.93	11.64	7.35	53.92
3	CO_2	7.93	4.30	1.70	0.4	54.22	8.83	5.04	68.10

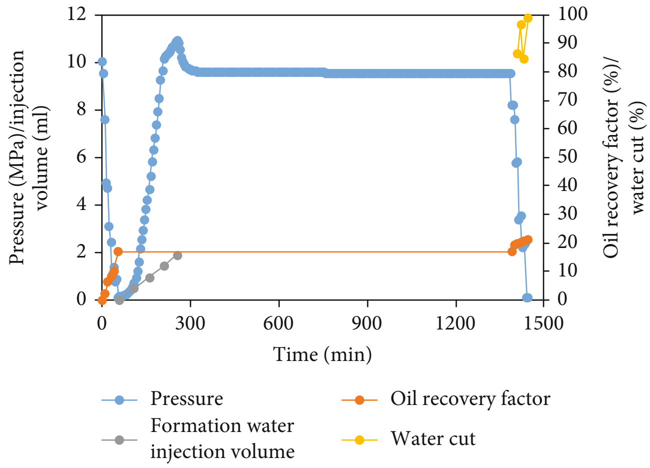

Figure 6: EOR performance of huff and puff by injecting formation water to original pressure + 0.2 PV (case 1).

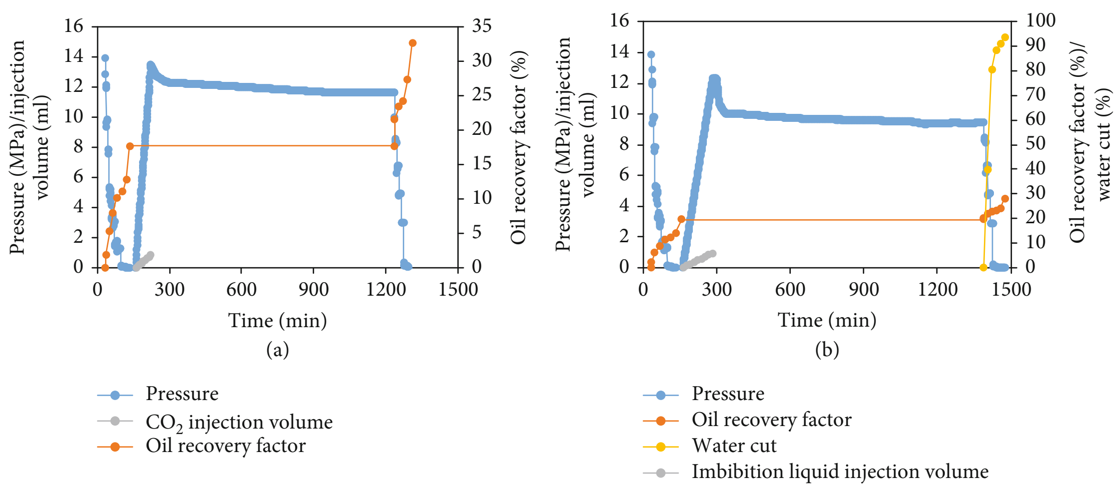

Figure 7: Comparison of EOR performance of huff and puff by injecting CO_2 and imbibition liquid to the original pressure: (a) huff and puff of CO_2 (case 2); (b) huff and puff of imbibition liquid SX-2 (case 5).

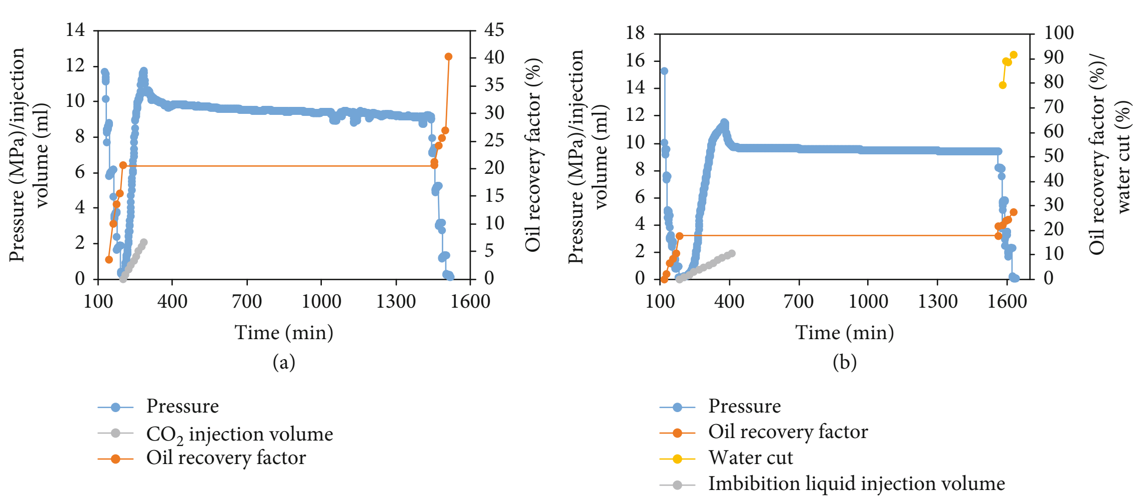

Figure 8: Comparison of EOR performance of huff and puff by injecting CO_2 and imbibition fluid to original pressure + 0.2 PV: (a) huff and puff of CO_2 (case 3); (b) huff and puff of imbibition liquid SX-2 (case 6).

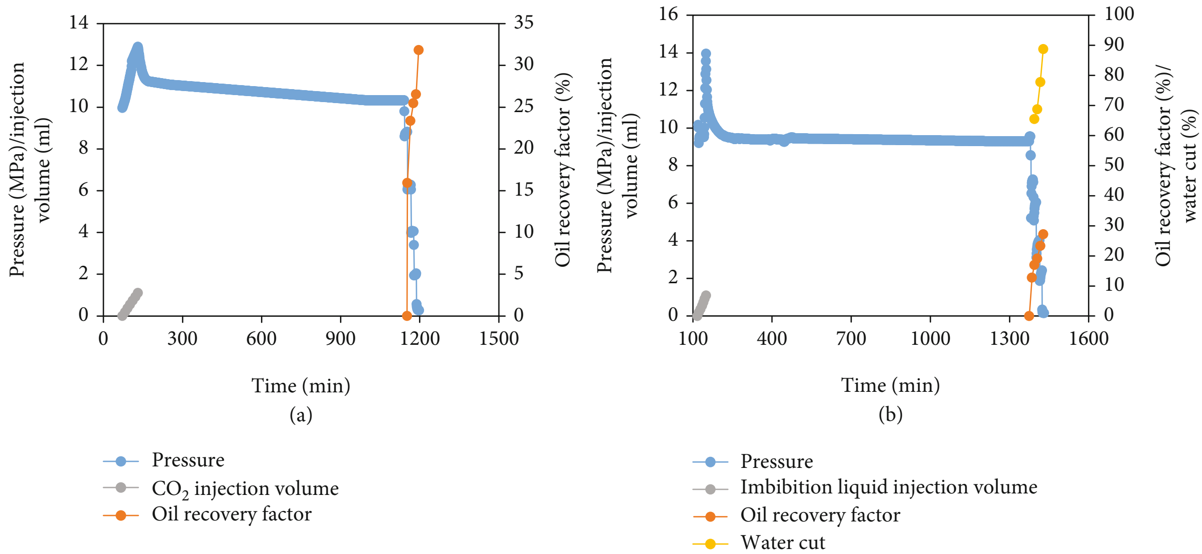

FIGURE 9: Comparison of EOR performance of huff and puff by directly injecting CO_2 and imbibition liquid at constant pressure: (a) huff and puff of CO_2 (case 4); (b) huff and puff of imbibition fluid SX-2 (case 7).

TABLE 8: Summary of huff and puff experimental results.

No.	Injected fluid	Injection volume	Recovery by depletion (%)	EOR by huff and puff (%)	Final recovery factor (%)	Oil-fluid ratio (ml/ml)
1	Formation water	To original pressure + 0.2 PV	16.99	4.24	21.23	0.1054
2	CO_2	To original pressure	17.62	15.07	32.70	1.8554
3	CO_2	To original pressure + 0.2 PV	20.59	19.75	40.34	0.9188
4	CO_2	0.2 PV	0	31.85	31.85	1.3661
5	Imbibition fluid SX-2	To original pressure	19.53	8.70	28.24	1.4457
6	Imbibition fluid SX-2	To original pressure + 0.2 PV	17.83	9.77	27.60	0.6708
7	Imbibition fluid SX-2	0.2 PV	0	27.18	27.18	1.1658

production (20.59%). In contrast, when the imbibition fluid SX-2 was injected for huff and puff, the final oil recovery factor was only 27.60%, increased by 9.77% on the basis of depletion production (17.83%), and the water cut of the produced fluid was 80-92%.

Cases 4 and 7 used the same procedures by directly injecting the CO_2 or imbibition liquid SX-2 into the core at constant pressure for huff and puff. As shown in Figure 9, the oil recovery factor of CO_2 huff and puff was 31.85%, while the oil recovery factor of huff and puff of imbibition liquid was 27.18%, associated with a water cut of 66-89%. In this huff and puff mode, the EOR performance of CO_2 and SX-2 becomes close.

For comparative analysis, the main results of huff and puff experiments are summarized in Table 8. It can be obtained that the EOR effect of CO_2 huff and puff is better than that of imbibition liquid. When the CO_2 or imbibition liquid is injected enough to restore the formation pressure to the original level, the injected fluid will be concentrated in the core near the inlet. So, the EOR performance in this case is relatively poor. Relatively, due to the strong dissolution and diffusion ability of CO_2 in crude oil, a better EOR performance of CO_2 can still be obtained (comparing cases 2 and 5). When an additional 0.2 PV of CO_2 or imbibition liquid is further injected after the core restoring to the original pressure, more injected fluid can migrate along the fractures to the deep formation and contact more oil-bearing reservoirs, which will result in a significant EOR performance when the well is opened for production (an additional EOR of 8.53% and 4.29% can be obtained by comparing cases 2 and 3 and comparing cases 5 and 6, respectively). When the huff and puff of CO_2 or imbibition liquid are carried out without depletion production, only a low oil recovery factor will be obtained despite the high oil-injected fluid ratio. The main reason for this is the lack of the depletion production process, in which the natural energy is not utilized.

To sum up, for the injection fluids of CO_2, imbibition liquid SX-2, and formation water, the oil recovery factor can be enhanced by 15.07-19.75%, 8.70-9.77%, and 4.24%, respectively, through the huff and puff. CO_2 is the best injection fluid for EOR, while imbibition liquids can be used to improve the imbibition ability of fracturing fluids. For the

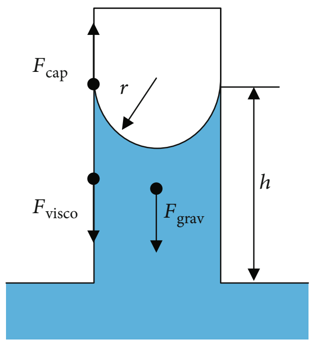

FIGURE 10: The forces acting on the water-phase liquid column in the pore during imbibition process.

huff and puff mode, the EOR performance in the mode of depletion production + pressure recovery + 0.2 PV is the best, while the oil-injected fluid ratio in the huff and puff mode of depletion production + pressure recovery is the largest (1.45-1.86 ml/ml). The EOR performance of CO_2 is more sensitive to the huff and puff mode than imbibition liquid.

3.4. Discussions

3.4.1. Imbibition Distance of Imbibition Liquid in Tight Oil Reservoirs. To estimate the imbibition distance of imbibition liquid in the fractured tight oil reservoirs, a simplified imbibition model was established based on the force analysis of the fluid in the pores. As shown in Figure 10, the water-phase liquid column in the tight core pores is affected by the capillary driving force, viscous force, and gravity. These forces can be expressed as follows [30]:

$$\text{Capillary driving force}: F_{cap} = \Delta p \pi r^2 = 2\sigma \cos \theta \pi r, \quad (1)$$

$$\text{Viscous force}: F_{visco} = 8\pi \mu h v, \quad (2)$$

$$\text{Gravity}: F_{grav} = \rho \pi r^2 h g, \quad (3)$$

$$\text{Momentum change}: F_m = \frac{d(mv)}{dt}, \quad \text{where } m = \rho \pi r^2 h, v = \frac{dh}{dt}. \quad (4)$$

The resultant of the first three forces should be equal to the momentum change during the spontaneous imbibition process, as follows:

$$F_m = F_{cap} - F_{visco} - F_{grav}, \quad (5)$$

where F_{cap}, F_{visco}, F_{grav}, and $d(mv)/dt$ are capillary driving force, viscous force, gravity, and momentum change, respectively (mN), Δp is the displacement pressure difference (mPa), r is the capillary radius (m), σ is the water-oil interface tension (mN/m), θ is the contact angle (°), μ is the viscosity of imbibition fluid (mPa·s), h is the imbibition height or distance (m), v is the velocity of imbibition fluid (m/s), ρ is the density of imbibition fluid (g/cm^3), g is the acceleration of gravity (m/s^2), m is the mass of imbibition fluid, and t is the imbibition time (s).

TABLE 9: Fitted parameters of imbibition model according to spontaneous imbibition experiment.

Case	E	Core	Physical properties
1	0.0185	27#	$\varphi = 2.7\%$
2	0.006	23#	$\varphi = 6.6\%$
8	0.22	D-4	$\varphi = 11.6\%$, $k = 0.606$ mD

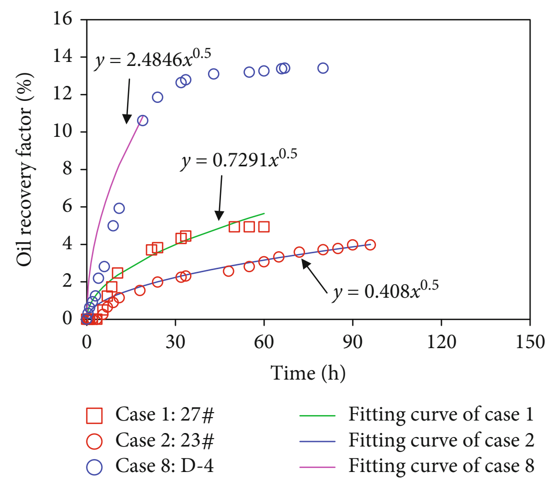

FIGURE 11: Fitting results of oil recovery factor in different spontaneous imbibition cases.

Substituting equations (1)–(4) into equation (5), the following equation can be obtained:

$$\frac{d}{dt}\left(\rho \pi r^2 h g \frac{dh}{dt}\right) = 2\sigma \cos \theta \pi r - 8\pi \mu h \frac{dh}{dt} - \rho \pi r^2 h g. \quad (6)$$

Neglecting the effect of fluid gravity and inertial force and assuming $\theta = 0°$ for simplification, we can get

$$0 = 2\sigma \pi r - 8\pi \mu h \frac{dh}{dt}. \quad (7)$$

By solving the above equation, the imbibition distance h can be expressed as follows:

$$h = \sqrt{\frac{\sigma r}{2\mu} t}. \quad (8)$$

Further, the imbibition velocity can be obtained:

$$v = 0.5\sqrt{\frac{\sigma r \cdot t^{-0.5}}{2\mu}}. \quad (9)$$

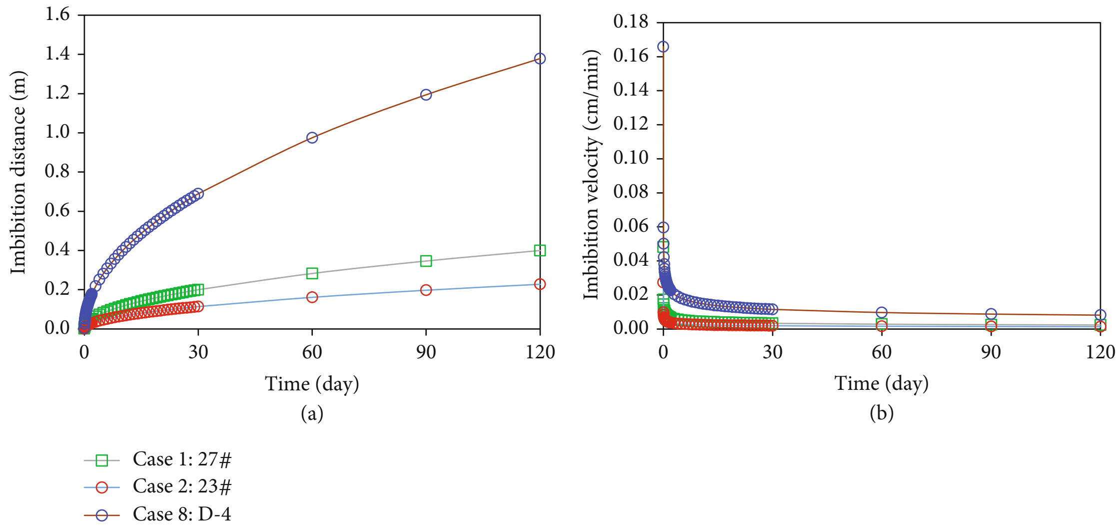

Figure 12: Predicted imbibition distance and velocity according to different spontaneous imbibition cases: (a) imbibition distance; (b) imbibition velocity.

According to the spontaneous imbibition experiment, the oil recovery factor can be expressed as follows:

$$\begin{aligned} \mathrm{RF} &= \frac{\text{Oil production}}{\text{Saturated oil volume}} = \frac{\text{Imbibed water volume}}{\text{Saturated oil volume}} \\ &= \frac{1/2 S_{\mathrm{core}} \phi h}{V_{\mathrm{core}} \phi S_o} = \frac{S_{\mathrm{core}}}{2 V_{\mathrm{core}} S_o} \sqrt{\frac{\sigma r}{2\mu} t}, \end{aligned} \tag{10}$$

where S_{core} is the surface area of the core (cm^2), V_{core} is the volume of core (cm^3), and S_o is the initial oil saturation.

Taking the typical spontaneous imbibition cases 1, 2, and 8 as examples, their oil recovery factors were fitted according to equation (10). The fitting results are shown in Table 9 and Figure 11.

Based on the fitting results, the imbibition distance and velocity of different cases were predicted according to equations (8) and (9). As shown in Figure 12, the imbibition distance increases with time and tends to reach stability. The imbibition distance of imbibition liquid SX-2 in the tight oil reservoir referring to core D-4 (case 8) is much larger than that of imbibition liquid SX-1 in the reservoirs referring to cores 23# and 27# (cases 1 and 2). Accordingly, the imbibition velocity of imbibition fluids at the beginning in the tight oil reservoirs is high, but it will decrease sharply and tends to be stable five days later. Overall, the imbibition distance and velocity of imbibition liquids are relatively small. The imbibition distance within 120 days is shorter than 1.4 m, and the maximum and stable imbibition velocities are no larger than 0.17 cm/min and 0.02 cm/min, respectively.

3.4.2. Diffusion Distance of CO_2 in Tight Oil Reservoirs. CO_2 transfers in crude oil by the diffusion mechanism. The diffusion coefficient of CO_2 in crude oil is a critical parameter for estimation of diffusion distance of CO_2 in the tight oil reservoirs, which can be calculated using the Wilkie formula neglecting the pore tortuosity for simplification [31]:

$$D_{\mathrm{A}} = \frac{7.4 \times 10^{-15} (\alpha M_{\mathrm{B}})^{0.5} T}{\mu_{\mathrm{slt}} {V_{\mathrm{A}}}^{0.6}}, \tag{11}$$

where D_{A} is the diffusion coefficient of solute A in liquid solvent B (m^2/s); M_{B} is the molar mass of solvent B (g/mol); α is the association coefficient of solvent B, when the solvent is water, $\alpha = 2.6$; when the solvent is an alkane, $\alpha = 1.0$; T is temperature (K); μ_{slt} is the viscosity of the solution (Pa s); and V_{A} is the liquid molar volume of solute A at the boiling point and normal pressure (cm^3/mol).

Taking $\alpha = 1$, $M_{\mathrm{B}} = 194$ g/mol, and $V_{\mathrm{A}} = 34\ \mathrm{cm}^3$/mol, the diffusion coefficient of CO_2 in crude oil was calculated and is shown in Table 10. It can be seen that as the CO_2 mole fraction in crude oil increases, the crude oil viscosity decreases. Accordingly, the CO_2 diffusion coefficient increases in a range of $(4.96\text{-}9.55) \times 10^{-9}\ \mathrm{m}^2/\mathrm{s}$. According to published studies [32, 33], the CO_2 diffusion coefficient in light oil usually varies in the order of magnitude ranging from 10^{-9} to $10^{-7}\ \mathrm{m}^2/\mathrm{s}$ in the porous media or bulk environments. Under stirring conditions, the CO_2 diffusion coefficient can even reach up to $10^{-6}\ \mathrm{m}^2/\mathrm{s}$.

The diffusion distance of CO_2 in crude oil can be calculated using the following equation, which was derived by Li et al. [32]:

$$\begin{aligned} C(x,t) = C_o - \frac{4C_o}{\pi} \sum_{n=0}^{\infty} \frac{1}{2n+1} \times \sin\left(\frac{(2n+1)\pi x}{2L_h}\right) \\ \times \exp\left(-\frac{(2n+1)^2 \pi^2 D_h}{4{L_h}^2} t\right), \end{aligned} \tag{12}$$

where $C(x,t)$ is the CO_2 concentration in crude oil at the distance x and time t (mol fraction), C_o is the equilibrium

Table 10: Calculated diffusion coefficients of CO_2 in tight oil (38 MPa, 150°C).

Mole fraction of CO_2 in oil	CO_2 solubility (sm^3/t)	Viscosity of crude oil (mPa·s)	CO_2 diffusion coefficient (10^{-9} m^2/s)
0	0	0.973	4.96
0.1	12.36	0.908	5.31
0.2	30.46	0.845	5.71
0.3	57.70	0.783	6.16
0.4	100.30	0.666	7.25
0.5	170.47	0.580	8.31
0.6	294.94	0.505	9.55

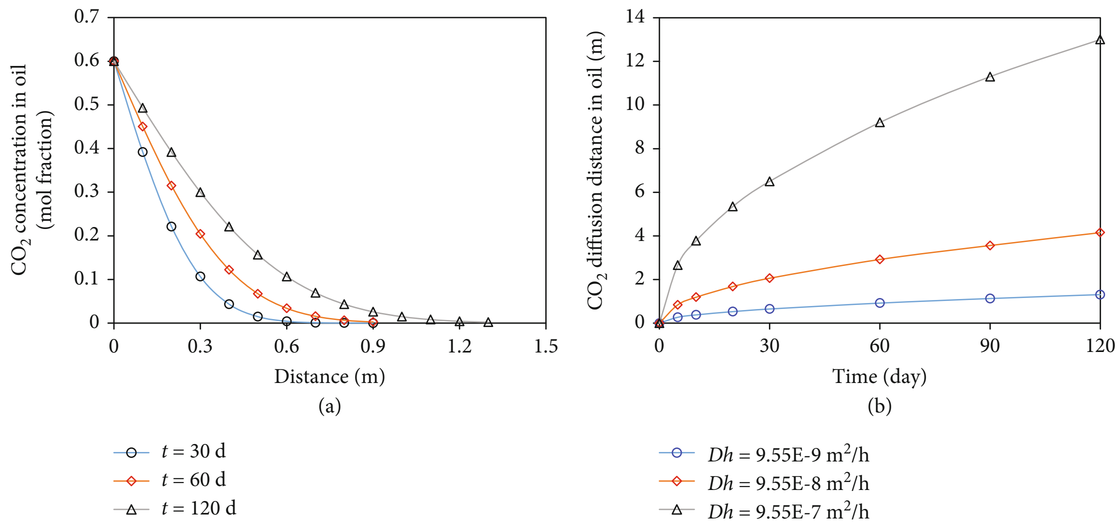

Figure 13: Predicted CO_2 diffusion concentration profile and distance in crude oil: (a) CO_2 diffusion concentration profile ($D_h = 9.55 \times 10^{-9}$ m^2/h); (b) CO_2 diffusion distances at different D_h.

concentration of CO_2 in crude oil at the distance 0 (mol fraction), x is the diffusion distance (m), t is time (s), D_h is the CO_2 diffusion coefficient (m^2/s), and L_h is the distance to the boundary (m).

The CO_2 concentration profiles in crude oil at different times and the CO_2 diffusion distances at different diffusion coefficients are shown in Figure 13. It can be seen that the concentration of CO_2 in crude oil decreases gradually with distance. When the CO_2 diffusion coefficient is 9.55×10^{-9} m^2/s, the diffusion distance of CO_2 in crude oil within 120 days will not be longer than 1.4 m. When the effective diffusion coefficient of CO_2 is enhanced 1-2 orders of magnitude by strong flowing or convention, the diffusion distance of CO_2 can be up to 4-13 m.

Compared with the imbibition liquids, CO_2 has a much larger penetration ability in tight rocks. CO_2 can affect the reservoir far away, while the imbibition liquid can affect the reservoir close to the well or fractures. When CO_2 and imbibition liquid are injected simultaneously or successively, more oil in the tight reservoirs will be produced out under the synergetic effect of these two fluids. These estimated imbibition/diffusion distance and velocity have a significant reference value, which can be used to estimate the enhanced sweeping volume of imbibition liquid during the soaking time. And after the imbibition liquid or CO_2 enters the fractures, under the condition that the imbibition distance of the imbibition liquid or the diffusion distance of CO_2 is certain, if the fracture spacing is large, the injected fluid cannot communicate well and cannot effectively displace the crude oil in the matrix. On the contrary, if the fracture spacing is small, the oil recovery factor can be better improved. Therefore, the evaluation of imbibition/diffusion distance is of great significance for determining fracture spacing. In addition, it also gives the other requirements of best parameters for hydraulic fracturing, such as the fracturing fluid composition and soaking time.

4. Conclusion

(1) Under spontaneous imbibition conditions, the imbibition effect of imbibition fluid SX-2 is the best, and the oil recovery factor of cores can be up to 13.416%. The tight and complete core is not conducive to the imbibition process, which will take a long time (60-100 h) to reach the total imbibition balance. The imbibition effect can play a more significant role in cracked cores. The imbibition fluid can contact more oil-bearing matrix through the cracks and displace oil by imbibition

(2) The dynamic imbibition and displacement experiments show that under reservoir conditions, when the injected CO_2 or imbibition fluids contact the matrix through fractures, CO_2 can penetrate the matrix through dissolution and diffusion in crude oil, while imbibition fluid can replace part of crude oil by imbibition effect. The displacement and imbibition effect (actually, it is dissolution, diffusion, and swelling effect) of CO_2 injection are better. The final oil recovery factor can reach 68.10%, which is 14.18% higher than that of imbibition fluid SX-2. When SX-2 is used as the injection fluid, a significant EOR can be obtained during production after well shut-in, with an increase ranging from 7.35% to 11.64%

(3) The huff and puff experiments show that the EOR performance of CO_2 huff and puff is better than that of imbibition fluid, and the EOR performance of huff and puff after depletion production is better than that of direct huff and puff. Injecting sufficient CO_2 or imbibition fluid can restore the formation pressure and contact more oil-bearing reservoirs along the fracture network, which can obtain a better EOR effect and increase the recovery factor by 4.29%-8.53%

(4) The imbibition and diffusion distances of imbibition fluids and CO_2 in tight oil reservoirs were estimated based on experimental fitting and theoretical calculation. The stable imbibition velocity of imbibition fluids is no larger than 0.02 cm/min, while the typical diffusion coefficient of CO_2 in tight cores is in an order of 10^{-9} m^2/s. Both the imbibition and diffusion distances of imbibition fluids and CO_2 are no more than 1.4 m within a 120-day soak time. When the diffusion coefficient of CO_2 is enhanced 1-2 orders of magnitude by flowing or convention, the diffusion distance of CO_2 can be up to 4-13 m. These estimated imbibition and diffusion velocities can provide guidance for the design of fracturing fluid, soak time, and fracture density for the on-site hydraulic fracturing

Data Availability

The datasets used or analyzed during the current study are available from the corresponding authors on reasonable request.

Conflicts of Interest

The authors declare that they have no conflicts of interest.

Acknowledgments

This research is supported by the Major National R&D Project: Key technologies of seismic and wellbore fine exploration (2016ZX05006-002) and the Natural Science Foundation of Shandong Province (ZR2020ME090).

References

[1] M. Dawson, D. Nguyen, and H. Li, "Designing an optimized surfactant flood in the Bakken," in *SPE/CSUR Unconventional Resources Conference*, SPE/CSUR, Calgary, 2015.

[2] Y. Su, B. Wang, N. Xu, Z. Zhang, Y. Liu, and J. Hou, "Discussion on energy storage fracturing technology of Chang X tight reservoir in block A of Dingbian area," *Petrochemical Industry Application*, vol. 39, no. 3, pp. 62–65 + 124, 2020.

[3] Z. Wei, X. Kang, X. Wang, D. Wang, and J. Zhang, "Enhanced oil recovery by wettability alteration method for tight reservoirs," *Science Technology and Engineering*, vol. 19, no. 23, pp. 107–112, 2019.

[4] H. Li, M. Dawson, and D. Standnes, "Multi-scale rock characterization and modeling for surfactant EOR in the Bakken," in *SPE/CSUR Unconventional Resources Conference*, SPE/CSUR, Calgary, 2015.

[5] C. Chen and M. Balhoff, "Effect of reservoir heterogeneity on improved shale oil recovery by CO_2 huff-n-puff," in *Society of Petroleum Engineers - SPE Unconventional Resources Conference*, Texas, 2013.

[6] T. Yang, Y. Zhang, Z. Yang, and T. Chen, "Mechanism of enhanced oil recovery by CO_2 flooding in tight sandstone reservoirs," *Science Technology and Engineering*, vol. 19, no. 24, pp. 113–118, 2019.

[7] Y. Wang, *Mechanism research of CO2 enhanced oil recovery for tight sand oil reservoir-take Yanchang formation 4+5 reservoir in an oil area of northern Shaanxi as an example*, Northwest University, 2019.

[8] P. Luo, W. Luo, and S. Li, "Effectiveness of miscible and immiscible gas flooding in recovering tight oil from Bakken reservoirs in Saskatchewan, Canada," *Fuel*, vol. 208, pp. 626–636, 2017.

[9] T. Lu, Z. Li, J. Li, D. Hou, and D. Zhang, "Flow behavior of N_2 huff and puff process for enhanced oil recovery in tight oil reservoirs," *Scientific Reports*, vol. 7, no. 1, p. 15695, 2017.

[10] J. Ma, X. Wang, R. Gao et al., "Enhanced light oil recovery from tight formations through CO_2 huff 'n' puff processes," *Fuel*, vol. 154, pp. 35–44, 2015.

[11] J. S. Qin and A. F. Li, *Reservoir Physics*, China University of Petroleum Press, 2003.

[12] D. S. Schechter, D. Zhou, and F. M. Orr Jr., "Low IFT drainage and imbibition," *Journal of Petroleum Science and Engineering*, vol. 11, no. 4, pp. 283–300, 1994.

[13] X. Yu, M. Zhang, L. He, W. Deng, L. Zhang, and H. Cao, "Influences of the clean fracturing flow-back fluid on the oil displaced effect of the spontaneous imbibition in dense reservoirs," *Daqing Petroleum Geology and Development*, vol. 38, no. 1, pp. 162–168, 2019.

[14] X. Liu, X. Chen, W. Liu, and X. Wang, "Influencing factors of dynamic imbibition displacement effect in tight sandstone reservoir and application," *Lithologic Reservoirs*, vol. 31, no. 5, pp. 114–120, 2019.

[15] M. Wang, S. Yang, Y. Cao, J. Wang, J. Yu, and W. Liu, "Mechanism of imbibition and oil recovery of fractured volcanic reservoir in Niudong," *Science and Technology and Engineering*, vol. 20, no. 2, pp. 569–575, 2020.

[16] L. Shun, N. Jun, W. Xianli et al., "A dual-porous and dual-permeable media model for imbibition in tight sandstone reservoirs," *Journal of Petroleum Science and Engineering*, vol. 194, p. 107477, 2020.

[17] J. Guo, M. Li, C. Chen, L. Tao, Z. Liu, and D. Zhou, "Experimental investigation of spontaneous imbibition in tight sandstone reservoirs," *Journal of Petroleum Science and Engineering*, vol. 193, p. 107395, 2020.

[18] Y. Sun, C. Dai, Y. Fang et al., "Imaging of oil/water migration in tightsand with nuclear magnetic resonance and microscope during dynamic surfactant imbibition," in *SPE-186240-MS Paper presented at the SPE/IATMI Asia Pacific Oil & Gas Conference and Exhibition*, Jakarta, 2017.

[19] P. Patil, N. Rohilla, A. Katiyar et al., "Surfactant based EOR for tight oil unconventional reservoirs through wettability alteration: novel surfactant formulations and their efficacy to induce spontaneous imbibition," in *SPE/AAPG/SEG Unconventional Resources Technology Conference*, Texas, 2018.

[20] F. Yu, H. Jiang, M. Ma, F. Xu, H. Su, and J. Jia, "Visualization the surfactant imbibition at pore scale by using of fractured micromodels," in *SPE Improved Oil Recovery Conference*, Tusla, 2020.

[21] J. Wang, S. Yang, Y. Cao, M. Wang, and J. Yu, "Imbibition mechanism of tight oil cores and experiments of surfactants enhancing oil recovery," *Science Technology and Engineering*, vol. 20, no. 3, pp. 1044–1050, 2020.

[22] X. Wang, J. Wu, F. Wu, and J. Yang, "Effect of surfactants on imbibition of low permeability reservoirs," *Petrochemical Industry*, vol. 48, no. 11, pp. 1157–1161, 2019.

[23] L. Zhang, C. Yang, B. Niu, and S. Ren, *EOR Principles and Application of CO_2 Flooding*, China University of Petroleum Press, Qingdao, 2017.

[24] L. Shi, Y. Zhang, H. Hu et al., "Adaptability analysis of supercritical CO_2 huff and puff in tight glutenite reservoir," *Science Technology and Engineering*, vol. 20, no. 9, pp. 3598–3604, 2020.

[25] X. Wang, M. N. Toksöz, and M. C. Fehler, "Laboratory and field-scale parameter optimization of CO_2 huff–n–puff with the staged-fracturing horizontal well in tight oil reservoirs," *Journal of Petroleum Science and Engineering*, vol. 186, 2020.

[26] Z. Song, Y. Song, Y. Li, B. Bai, K. Song, and J. Hou, "A critical review of CO_2 enhanced oil recovery in tight oil reservoirs of North America and China," *Fuel*, vol. 276, p. 118006, 2020.

[27] D. Du, W. Pu, F. Jin, and R. Liu, "Experimental study on EOR by CO_2 huff-n-puff and CO_2 flooding in tight conglomerate reservoirs with pore scale," *Chemical Engineering Research and Design*, vol. 156, pp. 425–432, 2020.

[28] Z. Liu, *The study on seepage regularity and imbibition enhanced oil recovery of tight sandstone Reservoirreservoir*, China University of Petroleum, Beijing, 2019.

[29] M. Yang, *Wettability alteration and Enhanced Oil Recovery of Surface-modification of SiO_2 nanoparticles*, China University of Petroleum, Beijing, 2019.

[30] P. Gao, *Experimental study on permeability and absorption characteristics of tight sandstone reservoir*, Xi'an Shiyou University, 2016.

[31] L. Zhang, *Saline aquifer storage of CO2 from natural gas reservoirs in the South China Sea: tfrapping mechanisms and project design*, China University of Petroleum (East China), 2011.

[32] D. Li, J. Hou, L. Zhao, P. Wang, and X. Yue, "Study on the molecular diffusion coefficient and solubility of carbon dioxide in crude oil," *Oilfield Chemistry*, vol. 26, no. 4, pp. 405–408, 2009.

[33] B. Guo, J. Hou, C. Yu, D. Li, and Y. Lin, "Determination of diffusion coefficient for CO2 in the porous media," *Journal of Petrochemical University*, vol. 22, no. 4, pp. 38–40, 2019.